Korean J. Chem. Eng., 37(2), 380-386 (2020)
DOI: 10.1007/s11814-019-0450-4

pISSN: 0256-1115
eISSN: 1975-7220

Polymerization of heterophasic propylene copolymer with $Me_2Si(2\text{-}Me\text{-}4\text{-}PhInd)_2ZrCl_2$ supported on SiO_2 and SiO_2-$MgCl_2$ carriers

Jade Dhalle Encarnacion, Sang Jun Park, and Young Soo Ko†

Department of Chemical Engineering, Kongju National University, Cheonan 31080, Korea
(*Received 23 September 2019 • accepted 1 December 2019*)

Abstract−$Me_2Si(2\text{-}Me\text{-}4\text{-}phInd)_2ZrCl_2$ supported on $SiO_2/MgCl_2$ binary support was prepared for the preparation of heterophasic copolymer of polypropylene. The bi-support underwent surface treatment with various alkyl aluminum compounds such as trimethylaluminum (TMA), triethylaluminum (TEAL), and triisobutylaluminum (TIBA) before supporting the metallocene catalyst for 3 or 24 hours and were used for homopolymerization. It was notable that the generated $SiO_2/MgCl_2$ bi-support had lower surface area, pore volume and size as compared to the conventional SiO_2. Impact polypropylene copolymers (IPCs) were obtained using two-step polymerization in one reactor with the presence of metallocene catalyst supported on SiO_2. Propylene was polymerized in the reactor to produce the iPP matrix followed by polymerization of ethylene resulting to heterophasic material. It is apparent that the molecular weight of the polymer increased with longer PE polymerization time and as the polymerization time was more than 40 min, PP peak appeared near 147.9-149.2 °C, and a new peak emerged at 116.9-119.9 °C which could be attributed to the melting temperature of iPP crystallites and a less intense peak to either chains of ethylene-propylene copolymers. SEM images also confirmed that spherical PE particles were deeply embedded in the crystalline PP matrix and a large amount was produced as the polymerization time of the second stage ethylene polymerization was increased.

Keywords: Metallocene Catalyst, $SiO_2/MgCl_2$ Bi-support, Aluminum Alkyl, Heterophasic Copolymerization

INTRODUCTION

Plastics have become one of the most universally used materials in industry and are essential in the global economy due to numerous applications [1]. Polypropylene (PP) is a multipurpose thermoplastic material with excellent mechanical properties. However, isotactic polypropylene (iPP) exhibits brittle behavior at low temperature under high loading rates [2]. To improve quality, polyethylene or other poly-alpha olefins, especially ethylene-propylene rubber (EPR), are blended to the iPP matrix.

Among the in reactor blending of iPP with other polyolefins, studies show that sequential polymerization is the most efficient method for impact strength improvement [3]. Due to the low cost and excellent impact properties, these materials are commercially known as impact polypropylene copolymers (IPCs) or heterophasic copolymer of polypropylene (HPC). This polymer is industrially produced in a two-step polymerization configuration with the presence of catalyst. During the first step, propylene is polymerized in the reactor to produce the iPP matrix followed by polymerization of ethylene and propylene gas mixture, resulting in heterophasic material that varies from amorphous and crystalline propylene-ethylene copolymers. Therefore, IPC makes excellent materials related to impact applications at low temperature due to its different crystalline and non-crystalline components. It covers a wide range of applications from trivial packaging uses to technically complex parts [4,5].

Moballegh et al. reported that additional polymerization was carried out after two-step PP/EPR polymerization at low ethylene concentration resulted in improvement of stiffness and impact strength resistance at low temperature [6]. Kakugo et al. investigated the morphology of Ziegler-Natta PP and heterophasic ethylene-propylene copolymer (HEPC) using SEM and TEM. After the first polymerization of propylene, the catalyst crystallites are dispersed uniformly in polymer particles. It has been reported that polymer particles are composed of polymer sub particles containing the catalyst crystallites as polymerization proceeds, and the ethylene-propylene copolymer is found at the boundary between particles [7]. Urdampilleta et al. compared the shape of PP homopolymer with that of HEPC containing 24% EPR and observed that copolymer was finely distributed in pores between PP matrix and mesoparticles [8]. However, there have been only a few reports on polymerization of HEPC with supported metallocene catalyst due to difficulty in its polymerization in a lab scale, though it has significant importance in polyolefin industries.

In this study, metallocene catalyst was loaded on the $SiO_2/MgCl_2$ binary support after surface treatment with different alkyl aluminum compounds. The synthesized metallocene bi-supported catalyst was used in the polymerization of ethylene and propylene, characterized using BET, ICP, XPS, and SEM in order to compare the different alkyl aluminum used. Furthermore, the SiO_2 supported catalysts were investigated in a two-step heterophasic PP copolymerization in only one reactor to obtain the IPC materials. In the first step of polymerization, polypropylene was introduced, then heterophasic PP copolymerization in which ethylene polymeriza-

†To whom correspondence should be addressed.
E-mail: ysko@kongju.ac.kr

tion was carried out in the second step. The obtained polymers were analyzed using DSC, GPC, and SEM. The catalytic performance was also observed by increasing the ethylene polymerization time.

EXPERIMENTAL

1. Materials

All chemicals were carried out under nitrogen atmosphere using the Schlenk technique. Silica (SP948, Grace) was calcined at 500 °C for 10 hours. Magnesium chloride ($MgCl_2$, Aldrich) was used without further treatment. Ethanol (Aldrich, 99.5%) and heptane (Aldrich, 99%) were used as received in $MgCl_2$ recrystallization. Dimethylsilyenebis(2-methyl-4-phenylindenyl)zirconium dichloride ($Me_2Si(2\text{-}Me\text{-}4\text{-}phInd)_2ZrCl_2$, PCI), methylaluminoxane (MAO, Albemarle), trimethylaluminum (TMA, Aldrich), triethylaluminum (TEAL, Aldrich) and triisobutylaluminum (TIBAL, Aldrich) were used without further purification. Toluene and hexane from J.T Baker were purified by refluxing with sodium metal and benzophenone in a nitrogen atmosphere. Ethylene (99.999%), propylene (SK energy, Korea, 99.999%) and nitrogen (AIR PRODUCTS, Korea, 99.999%) were passed through Fisher's REDOX Oxygen Removal Tube and 5A/13AX molecular sieve to remove moisture and oxygen.

2. Catalyst Synthesis

2-1. $SiO_2/MgCl_2$ Binary Support Synthesis

In 10 mL of heptane, 1 g of $MgCl_2$ was slurried and 4.3 mL of ethanol was added. The suspension was stirred at 89 °C for 1 hour, then 2 g of SiO_2 suspended in 30 mL of heptane at 89 °C was added. The reaction proceeded for 1 hour at 89 °C with vigorous stirring. To synthesize $SiO_2/MgCl_2$ binary support, the resultant mixture was washed four times with heptane at 70 °C and dried under vacuum at 40 °C for 1 hour.

2-2. Surface Treatment of Binary Support Using Alkyl Aluminum Compound

In a 30 mL toluene, 1 g of $SiO_2/MgCl_2$ binary support was suspended at 0 °C with ice and water, then a suitable amount of cocatalyst alkyl aluminum compound was added. The reaction proceeded for 2 hours at 0 °C. After the reaction completion, the catalyst was washed with toluene five times and dried under vacuum at 40 °C for 1 hour to synthesize $SiO_2/MgCl_2$/alkyl aluminum support.

2-3. Supporting the Catalyst

0.1 mmol of $Me_2Si(2\text{-}Me\text{-}4\text{-}phInd)_2ZrCl_2$ and 20 mmol of MAO solution in toluene were added to 1 g of $SiO_2/MgCl_2$/alkyl aluminum support suspended in toluene. The reaction proceeded for 3 or 24 hours at 50 °C with vigorous stirring. The catalyst was washed five times using toluene after the reaction was completed and dried under vacuum at 40 °C for 1 hour to synthesize $SiO_2/MgCl_2$/alkyl aluminum/$Me_2Si(2\text{-}Me\text{-}4\text{-}phInd)_2ZrCl_2$.

3. Polymerization

3-1. Polymerization of Ethylene and Propylene

The ethylene and propylene polymerization were carried out in a 500 mL steel high-pressure reactor equipped with mechanical stirrer for agitation. 280 mL of hexane and 2 mmol of TEAL as cocatalyst were introduced to the reactor. The temperature was increased to 50 °C, then a certain amount of catalyst in a slurry state with 5 mL of hexane was added. After a total pressure of 7 bar was maintained and the reactor was saturated with monomers, the polymerization was started with stirring. The resulting polymer was washed with ethanol, vacuum filtered and dried.

3-2. Heterophasic PP Copolymerization

The heterophasic PP copolymerization was carried out in a 500 mL steel high-pressure reactor equipped with mechanical stirrer for agitation. 280 mL of hexane and 2 mmol of TEAL as cocatalyst were introduced to the reactor. The temperature was increased to 50 °C, followed by the addition of 100 mg of catalyst in a slurry state with 5 mL of hexane. The polymerization of propylene started with stirring after the monomer was saturated and a pressure of 7 bar was achieved. After the polymerization, the temperature was reduced to 30 °C. The unreacted propylene was discharged to the atmosphere and was purged three times with ethylene, then the temperature was increased to 50 °C. The ethylene polymerization was started with agitation and a pressure of 3 bar was maintained during the reaction. The resulting polymer was washed with ethanol, vacuum filtered and dried.

4. Characterization

The surface area of the supports and catalysts used in the experiments was measured by Micromeritics ASAP 2010 instrument and was calculated by the Brunauer-Emmett-Teller (BET) equation. The sample was dried before measurement and then outgassed under vacuum for 12 hours at 150 °C. The Mg, Al, and Zr content in the supported catalysts was measured by inductively coupled plasma atomic emission spectroscopy (Perkin-Elmer, Optima 200DV). Using X-ray photoelectron spectroscopy (XPS), the binding energies of Zr supported on the carrier were measured. To obtain DSC curves, the melting point of the resulting polymer was measured by differential scanning calorimetry (DSC, TA 2010) at a rate of 10 °C/min at 25 °C to 180 °C. The molecular weight and molecular weight distribution of the resulting polymer were determined by GPC (Waters Associates Chromatograph, Model ALC-GPC-150C) analysis. The morphology of the support, catalysts, and resulting polymer was observed through a field emission scanning electron microscope (FE-SEM, TESCAN, MIRA LMH).

RESULTS AND DISCUSSION

1. Characterization of $SiO_2/MgCl_2$ Binary Support and Supported Catalyst

In the absence of surface treatment, both the catalytic performance and degree of impregnation are usually low if the metallocene catalyst is directly impregnated on a support [9]. This study explored generating the $SiO_2/MgCl_2$ binary support by using $MgCl_2$ in hexane, then dissolving in ethanol and supporting on SiO_2. Since alcohol deactivates metallocene catalyst, the $SiO_2/MgCl_2$ binary support was surface treated with different alkyl aluminum to eliminate the residual ethanol [10].

As can be seen in Table 1, $SiO_2/MgCl_2$ binary carrier and supported catalysts having a reaction time of 24 hours were investigated using BET and ICP analysis. The $SiO_2/MgCl_2$ binary support has lower surface area, pore volume and size as compared to the conventional SiO_2 due to the presence of recrystallized $MgCl_2$ on it. Upon the surface treatment of the $SiO_2/MgCl_2$ binary support

Table 1. Physical properties and chemical composition of $SiO_2/MgCl_2$ supported catalyst

Sample	BET analysis			ICP analysis		
	Surface area (m^2/g)	Pore volume (cm^3/g)	Pore size (nm)	Mg content (mmol/g-cat)	Al content (mmol/g-cat)	Zr content (μmol/g-cat)
$MgCl_2$	3	0.02	9.3	9.5	-	-
SiO_2	274	1.63	18.9	-	-	-
$SiO_2/MgCl_2$	188	1.02	16.2	2.3	-	-
$SiO_2/MgCl_2$/TMA	164	0.90	17.0	2.3	0.9	-
$SiO_2/MgCl_2$/TEAL	181	0.97	16.9	2.3	0.7	-
$SiO_2/MgCl_2$/TIBAL	182	0.97	17.4	2.3	0.7	-
$SiO_2/Me_2Si(2\text{-Me-4-phInd})_2ZrCl_2$/MAO	199	0.94	16.0	-	6.5	45.8
$SiO_2/MgCl_2$/TMA/$Me_2Si(2\text{-Me-4-phInd})_2ZrCl_2$/MAO	164	0.77	16.1	2.2	3.5	16.8
$SiO_2/MgCl_2$/TEAL/$Me_2Si(2\text{-Me-4-phInd})_2ZrCl_2$/MAO	184	0.86	16.2	2.3	3.0	14.8
$SiO_2/MgCl_2$/TIBAL/$Me_2Si(2\text{-Me-4-phInd})_2ZrCl_2$/MAO	179	0.75	14.8	2.1	3.0	18.5

with alkyl aluminum compound and metallocene catalyst the surface area declined. This suggested that the recrystallize $MgCl_2$ and alkyl aluminum on SiO_2 caused a reduction of the surface area [11].

It can be observed that the Al content of the resulting catalysts was significantly increased. This is due to the addition of MAO. In the impregnation of the metallocene catalyst on the support, MAO is known to be a co-catalyst that acts as an anchor between metallocene and silica for its surface modification [12]. In addition, $SiO_2/Me_2Si(2\text{-Me-4-phInd})_2ZrCl_2$/MAO catalyst has the largest surface area than $SiO_2/MgCl_2$ bi-supported catalysts, which could be attributed to more Al and Zr content.

$SiO_2/MgCl_2$/TIBAL/$Me_2Si(2\text{-Me-4-phInd})_2ZrCl_2$/MAO, which has the larger surface area compared to the most alkyl aluminum treated $SiO_2/MgCl_2$ bi-supported catalysts, resulted in highest Zr content. According to Ko et al., TIBAL has a bulky molecular size which can be used for more porous sites for immobilization of zirconocene [13].

In addition, ICP analysis confirmed that more than twice as much of the Zr content of the catalyst can be carried on SiO_2 which is 45.8 μmol/g-cat than $SiO_2/MgCl_2$/alkyl aluminum. Since SiO_2 supported catalyst has the largest surface area and highest Al content on the surface, that improved the metallocene catalyst impregnation [14].

To increase the Zr content on the support, the catalyst was synthesized by extending the stirring time. Gauthier et al. proposed that to make the metallocene become reactively supported on the carrier material with the aluminoxane, it was desirable to maintain the agitation for a period of one or more hours [15]. The Zr content of the catalyst prepared by stirring for 3 hours was 15.1 μmol/g-cat, while the Zr content of the catalyst by stirring for 24 hours was 18.5 μmol/g-cat.

Fig. 1 illustrates the XPS Zr 3d analysis of the $Me_2Si(2\text{-Me-4-phInd})_2ZrCl_2$ and the supported catalysts. The Zr binding energy peaks of the metallocene catalyst and SiO_2 supported catalyst were measured in the range of 184.4-184.3 eV (Zr $3d_{5/2}$) and 182.0-182.2 eV (Zr $3d_{3/2}$), respectively. Similar behavior can be found in the literature for the binding energy of Zr 3d of $Me_2Si(2\text{-Me-4-phInd})_2ZrCl_2$ and known to be around 182.70 eV, while supporting it to

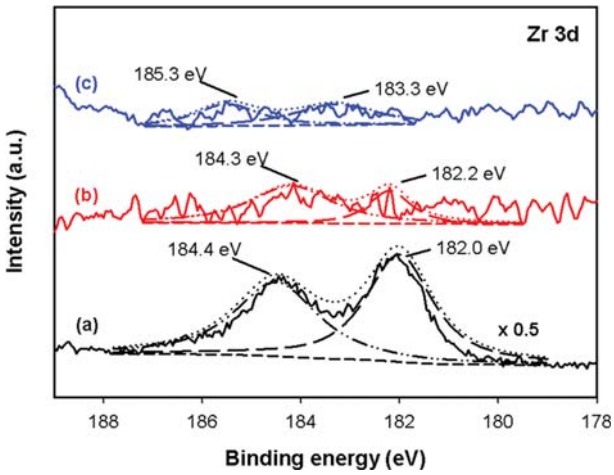

Fig. 1. The XPS Zr 3d spectra of (a) $Me_2Si(2\text{-Me-4-PhInd})_2ZrCl_2$, (b) $SiO_2/Me_2Si(2\text{-Me-4-PhInd})_2ZrCl_2$/MAO and (c) $SiO_2/MgCl_2$/TMA/$Me_2Si(2\text{-Me-4-PhInd})_2ZrCl_2$/MAO.

SiO_2 shifts the binding energy to a higher value [16-18]. Previous studies have emphasized the existence of a more electron deficient species resulting in a higher binding energy due to the electronic environment difference from the substitution between an oxygen atom from silica and chlorine atom from zirconocene. Furthermore, the Zr binding energy of the metallocene catalyst supported $SiO_2/MgCl_2$/alkyl aluminum compound employed a slightly higher Zr binding energy than $Me_2Si(2\text{-Me-4-phInd})_2ZrCl_2$ [19], which is 185.3 eV (Zr $3d_{5/2}$) and 183.3 eV (Zr $3d_{3/2}$), respectively.

The morphology of the catalysts synthesized was examined by SEM as presented in Fig. 2. SEM images portrayed that there were some occurrences of catalyst breakages. Particle size of supporting the metallocene catalyst on $SiO_2/MgCl_2$/alkyl aluminum is smaller than the SiO_2 supported catalyst [20]. The possible reason might be the longer stirring time of synthesizing the catalyst. It can be confirmed that the bi-supported catalyst was rough with the agglomeration of $MgCl_2$. Several authors have reported that reaction between the bi-support and alkyl aluminum compound resulted in

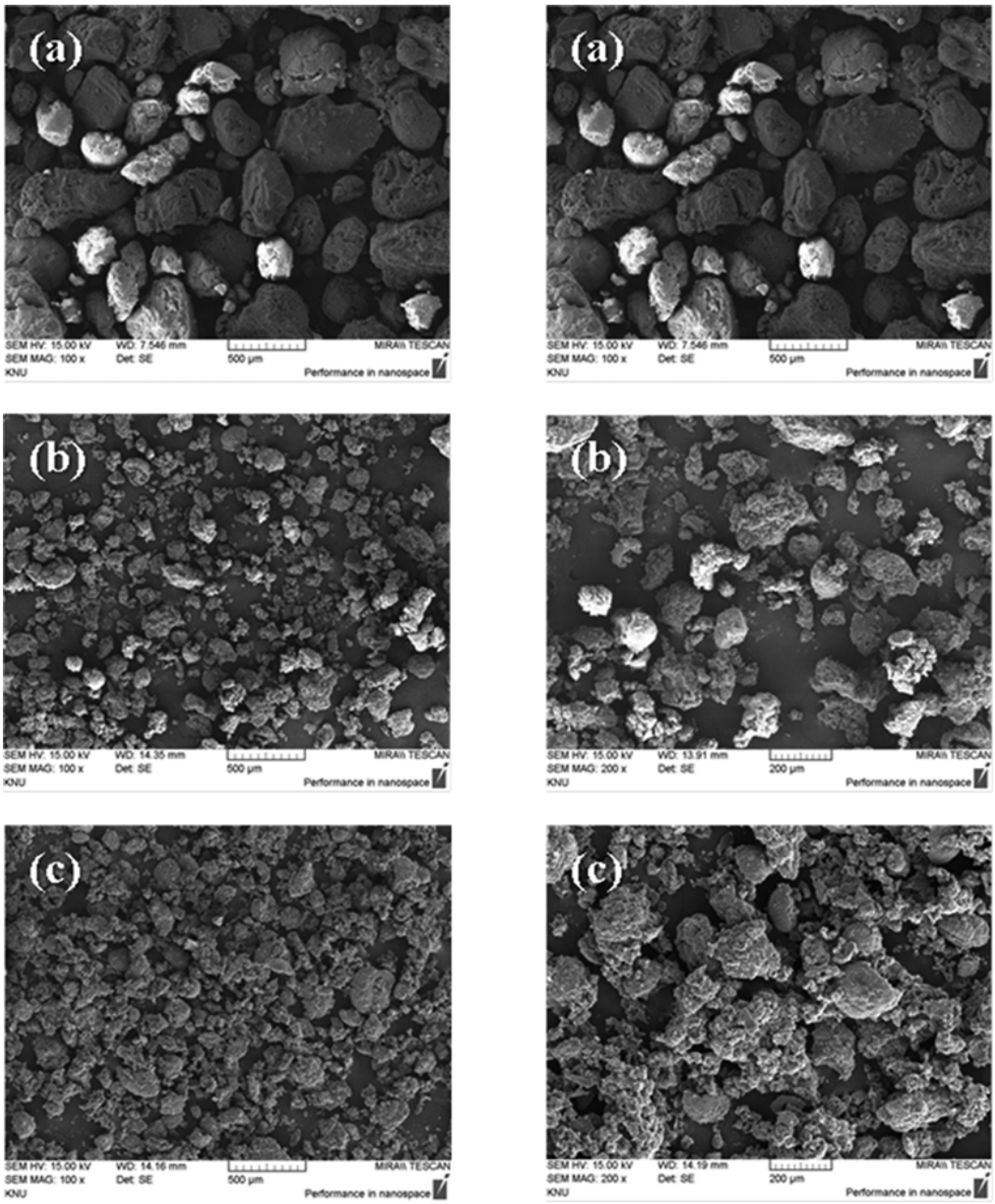

Fig. 2. SEM images of (a) $SiO_2/Me_2Si(2\text{-}Me\text{-}4\text{-}phInd)_2ZrCl_2$/MAO, (b) $SiO_2/MgCl_2$/TMA/$Me_2Si(2\text{-}Me\text{-}4\text{-}phInd)_2ZrCl_2$/MAO and (c) $SiO_2/MgCl_2$/TIBAL/$Me_2Si(2\text{-}Me\text{-}4\text{-}phInd)_2ZrCl_2$/MAO.

fractured and reduced particle size [14,20].

2. Ethylene and Propylene Polymerization of Catalyst

The data obtained from ethylene and propylene polymerization are summarized in Tables 2 and 3, respectively. Catalysts used in the polymerization were synthesized by mixing the metallocene catalyst and MAO with $SiO_2/MgCl_2$/alkyl aluminum support for 3 or 24 hours.

For ethylene polymerization, metallocene catalyst supported on SiO_2 yielded higher activity than $SiO_2/MgCl_2$/alkyl aluminum supported catalyst. The influence of various alkyl aluminum compounds on the surface treatment of $SiO_2/MgCl_2$ binary support was evaluated by synthesizing the catalyst for 24 hours. The activity of the catalyst supported on the bi-support can be determined by the following equation: $SiO_2/MgCl_2$/TMA/$Me_2Si(2\text{-}Me\text{-}4\text{-}phInd)_2ZrCl_2$> $SiO_2/MgCl_2$/TIBAL/$Me_2Si(2\text{-}Me\text{-}4\text{-}phInd)_2ZrCl_2$>$SiO_2/MgCl_2$/TEAL/$Me_2Si(2\text{-}Me\text{-}4\text{-}phInd)_2ZrCl_2$. Similar observation in the ethylene polymerization has been previously reported in the literature. It attested that the catalyst pretreated with TMA shows a higher activity compared to the catalyst pretreated with TIBAL and no polymerization activity was observed upon pretreatment with TEAL [21]. It is notable that surface treatment of $SiO_2/MgCl_2$ with alkyl aluminum causes steric hindrance to the diffusion of ethylene monomer [22]. In addition, alkyl aluminum form complexes with active zirconium occupy the vacant coordinate sites and lessen the active

Table 2. Results of ethylene polymerization with $Me_2Si(4\text{-}Ph\text{-}2\text{-}MeInd)_2ZrCl_2$ supported on $SiO_2/MgCl_2$

Catalysts[a]	Stirring time (h)	Cat. (mg)	PE (g)	Activity Kg-PE/(mmol-Zr*h)	T_m (°C)	ΔH_f (J/g)
$SiO_2/Me_2Si(2\text{-}Me\text{-}4\text{-}phInd)_2ZrCl_2/MAO$	3	40	21.1	4.6	133.5	164.8
$SiO_2/MgCl_2/TMA/Me_2Si(2\text{-}Me\text{-}4\text{-}phInd)_2ZrCl_2/MAO$	24	100	7.4	4.4	132.5	129.7
$SiO_2/MgCl_2/TIBAL/Me_2Si(2\text{-}Me\text{-}4\text{-}phInd)_2ZrCl_2/MAO$	3	40	3.2	2.1	132.8	151.0
		100	6.3	4.2	132.6	133.4
	24	100	7.5	4.1	132.5	154.9
$SiO_2/MgCl_2/TEAL/Me_2Si(2\text{-}Me\text{-}4\text{-}phInd)_2ZrCl_2/MAO$	24	100	2.5	1.7	133.5	141.4

[a]Polymerization condition: TEAL in feed=2 mmol, ethylene pressure=7 bar, temperature=50 °C, time=1 h

Table 3. Results of propylene polymerization with $Me_2Si(4\text{-}Ph\text{-}2\text{-}MeInd)_2ZrCl_2$ supported on $SiO_2/MgCl_2$

Catalysts[a]	Stirring time (h)	PP (g)	Activity kg-PP/(mmolZr*h)	T_m (°C)	ΔH_f (J/g)
$SiO_2/Me_2Si(2\text{-}Me\text{-}4\text{-}phInd)_2ZrCl_2/MAO$	3	11	2.4	148.9	78.0
$SiO_2/MgCl_2/TMA/Me_2Si(2\text{-}Me\text{-}4\text{-}phInd)_2ZrCl_2/MAO$	24	1	-	147.9	69.3
$SiO_2/MgCl_2/TIBAL/Me_2Si(2\text{-}Me\text{-}4\text{-}phInd)_2ZrCl_2/MAO$	3	0.1	-	145.8	35.8
	24	0.6	-	149.1	62.4

[a]Polymerization condition: cat.=100 mg, TEAL in feed=2 mmol, propylene pressure=7 bar, temperature=50 °C, time=1 h

Table 4. Results of heterophasic PP copolymerization with $SiO_2/Me_2Si(2\text{-}Me\text{-}4phInd)_2ZrCl_2$

Catalysts[a]	PP	PE		PP-b-PE	Activity	PP		PE		M_n	PDI
	(g)	Pressure (bar)	Time (min)	(g)	kg-PP/ (mmol-Zr*h)	T_m (°C)	ΔH_f (J/g)	T_m (°C)	ΔH_f (J/g)	(g/mol)	
$SiO_2/Me_2Si(2\text{-}Me\text{-}4\text{-}phInd)_2ZrCl_2/MAO$	11	-	-	-	2.4	148.9	78.0	-	-	57700	6.8
	-	3	5	14.1	-	149.2	87.9	-	-	-	-
			10	19.4	-	147.9	63.4	-	-	-	-
			20	23.7	-	148.7	65.2	-	-	28200	8.3
			40	31.3	-	148.6	35.0	116.9	8.5	33700	8.5
			60	34.6	-	148.5	27.0	119.9	29.0	48800	5.8

[a]Polymerization condition: cat.=100 mg, TEAL in feed=2 mmol, propylene pressure=7 bar, temperature=50 °C, time=1 h

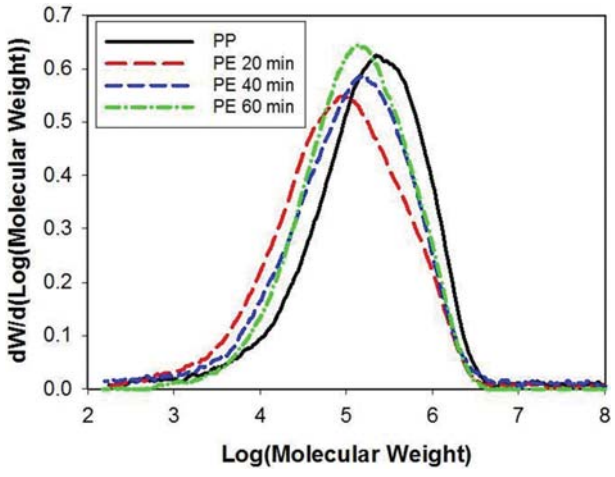

Fig. 3. GPC curves for heterophasic PP copolymer.

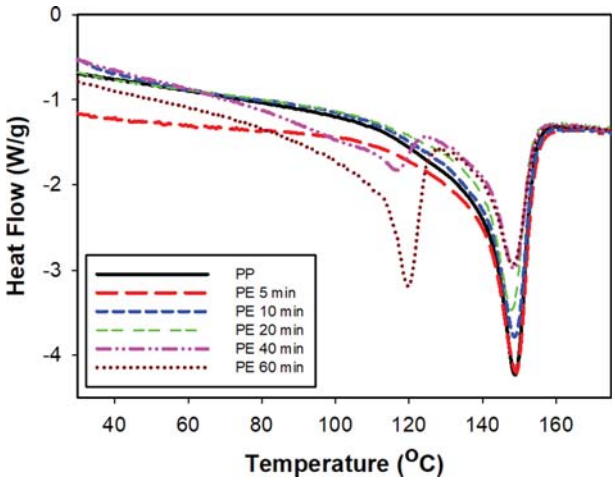

Fig. 4. DSC curves of different polyethylene polymerization time.

sites for polymerization [23].

In propylene polymerization, only traces of the PP can be found for catalysts having surface treated with various alkyl aluminum compounds and metallocene supported on $SiO_2/MgCl_2$ binary sup-

port compared to the catalyst supported on SiO_2 which has an activity of 2.4 kg-PP/(mmol-Zr*h).

3. Heterophasic PP Copolymerization

To generate EPR elastomeric materials embedded in the iPP matrix, the second step polymerization process was performed. Ethylene-propylene comonomers were fed to the reactor.

The results of GPC analysis of the homopolymerization of propylene and heterophasic PP copolymerization are shown in Table 4 and Fig. 3. The molecular weight of polymer produced by PP polymerization was 57,700 g/mol, which is higher than the heterophasic copolymers. In heterophasic PP copolymerization, it is apparent that the molecular weight of the polymer increased with longer PE polymerization time. This can be attributed to the fact that more ethylene content is incorporated in the PP matrix as the second stage ethylene polymerization time increases. The results substantiate previous findings in the literature that controlling the copolymerization time achieved different amount of ethylene and mechanical properties. Moreover, a higher ethylene in EPR has

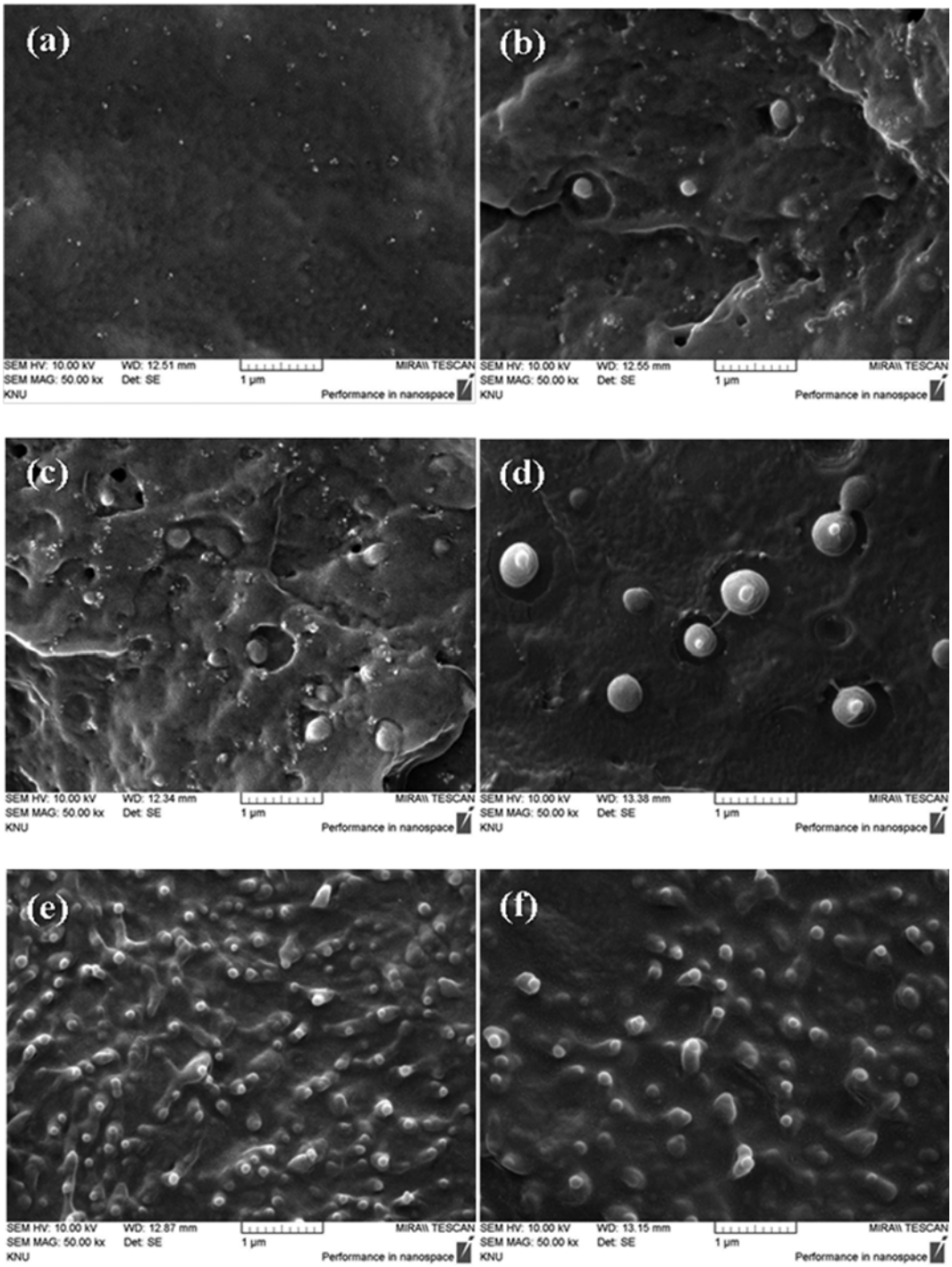

Fig. 5. SEM images of (a) PP, (b) PE 5 min, (c) PE 10 min, (d) PE 20 min, (e) PE 40 min and (f) PE 60 min.

proven to be a key factor in excellent toughness-stiffness balance of in-reactor mixtures [24].

On the other hand, the melting point was determined by DSC shown in Table 4 and Fig. 4. As the ethylene content increased, the PP peak appeared near 147.9-149.2 °C, and a new peak emerged at 116.9-119.9 °C when the second stage ethylene polymerization time was more than 40 minutes. This showed that PE peaks with low melting points appear as the ethylene content rises. Previous studies have documented the two main peaks contributions, which are assigned to the melting temperature of iPP crystallites, and a less intense peak that could be attributed to the either chains of ethylene-propylene copolymers [25,26].

To determine the morphology of the different heterophasic copolymers, an SEM experiment was conducted. Fig. 5 shows SEM images of the surface of the polymer after it was frozen with liquid nitrogen. It was confirmed that spherical PE particles are deeply embedded in the crystalline PP matrix and a large amount is produced as the polymerization time of the second stage ethylene polymerization is increased. In addition, gradual smoothing of the surface can be detected at longer reaction time of ethylene polymerization and it was coated completely with ethylene layer [27].

CONCLUSION

$SiO_2/MgCl_2$ binary support was successfully synthesized, surface treated with different alkyl aluminum and then loaded with metallocene catalyst $Me_2Si(2\text{-}Me\text{-}4\text{-}phInd)_2ZrCl_2$. The supported catalysts were used in homopolymerization and heterophasic PP copolymerization. Taken together, the results suggest that alkyl aluminum compound used in surface treatment lowered the catalytic performance. This paper also highlights the effect of prolonging the PE polymerization time in heterophasic PP copolymerization using the metallocene catalyst supported on SiO_2. An increase in molecular weight and a presence of PE peak with lower melting point can be depicted with escalating the ethylene content, as would be expected.

ACKNOWLEDGEMENTS

This work was supported by a National Research Foundation of Korea (NRF) grant funded by the Korean government (MSIP) (2016R1D1A1B01009941). This work was also supported by the Human Resources Program in Energy Technology of the Korea Institute of Energy Technology Evaluation and Planning (KETEP), granted financial resource from the Ministry of Trade, Industry & Energy, Republic of Korea (No. 20194010201730).

REFERENCES

1. M. T. P. García, I. Suárez, M. T. Expósito, B. Coto and R. García-Muñoz, *Eur. Polym. J.*, **93**, 436 (2017).
2. R. García, B. Coto, M.-T. Expósito, I. Suarez, A. Fernández-Fernández and S. Caveda, *Macromol. Res.*, **19**, 778 (2011).
3. M. T. Pastor-García, I. Suárez, M. T. Expósito, B. Coto and R. García-Muñoz, *Eur. Polym. J.*, **106**, 156 (2018).
4. L. Botha and A. van Reenen, *Eur. Polym. J.*, **49**(8), 2202 (2013).
5. K. Kruczala, J. G. Bokria and S. Schlick, *Macromolecules*, **36**(6), 1899 (2003).
6. L. Moballegh, S. Hakim, J. Morshedian and M. Nekoomanesh, *J. Polym. Res.*, **22**(5), 1 (2015).
7. M. Kakugo, H. Sadatoshi, J. Sakai and M. Yokoyama, *Macromolecules*, **22**(7), 3172 (1989).
8. I. Urdampilleta, A. González, J. J. Iruin, J. C. de la Cal and J. M. Asua, *Macromolecules*, **38**(7), 2795 (2005).
9. K. Soga and M. Kaminaka, *Macromol. Rapid Commun.*, **13**, 221 (1992).
10. H. S. Cho and W. Y. Lee, *Korean J. Chem. Eng.,* **19**(4), 557 (2002).
11. A. C. Cariño, S. J. Park and Y. S. Ko, *Appl. Chem. Eng.*, **29**, 461 (2018).
12. H. S. Cho, K. H. Choi, D. J. Choi and W. Y. Lee, *Korean J. Chem. Eng.,* **17**(2), 205 (2000).
13. Y. G. Ko, H. S. Cho, K. H. Choi and W. Y. Lee, *Korean J. Chem. Eng.*, **16**(5), 562 (1999).
14. J. S. Chung, H. S. Cho, Y. G. Ko and W. Y. K. Lee, *J. Mol. Catal. A: Chem.*, **144**(1), 61 (1999).
15. W. J. Gauthier, M. Lopez, D. J. Rauscher, D. G. Campbell, Jr. and M. E. Kerr, Method for the preparation of metallocene catalysts, United States Patent US6777366B2 (2004).
16. F. Garbassi, L. Gila and A. Proto, *J. Mol. Catal. A: Chem.*, **101**, 199 (1995).
17. F. Silveira, D. Santos de Sa, Z. Novais da Rocha, M. do Carmo, M. Alves and J. H. Zimnoch dos Santos, *X-Ray Spectrom.*, **37**, 615 (2008).
18. M. Atiqullah, M. Faiz, N. Akhtar, M. A. Salim, S. Ahmed and J. H. Khan, *Surf. Interface Anal.*, **27**, 728 (1999).
19. R. F. Jordan, *Adv. Organomet. Chem.*, **32**, 325 (1991).
20. S. Patthamasang, B. Jongsomjit and P. Praserthdam, *Molecules*, **16**, 8332 (2011).
21. S. Sensarma and S. Sivaram, *Polym. Int.*, **51**, 417 (2002).
22. H.-x. Zhang, Y.-j. Lee, J.-r. Park, D.-h. Lee and K.-B. Yoon, *Polym. Bull.*, **67**(8), 1519 (2011).
23. H. S. Cho, J. S. Chung, Y. G. Ko, K. H. Choi and W. Y. Lee, *Sci. Technol. Catal.*, **121**, 481 (1999).
24. Y. Fan, C. Zhang, Y. Xue, W. Nie and X. Zhang, *Polym. J.*, **41**, 1098 (2009).
25. R. A. García, B. Coto, M.-T. Expósito, I. Suarez, A. Fernández-Fernández and S. Caveda, *Macromol. Res.*, **19**, 778 (2011).
26. B. M. Huerta-Martínez, E. Ramírez-Vargas, F. J. Medellín-Rodríguez and R. C. Garcia, *Eur. Polym. J.*, **41**, 519 (2005).
27. L. Botha and A. van Reenen, *Eur. Polym. J.*, **49**, 2202 (2013).